Jordanian Journal of Computers and Information Technology (JJCIT), Vol. 05, No. 02, August 2019.

LOW PASS AND QUAD BAND PASS TUNABLE FILTER BASED ON STUB RESONATOR TECHNIQUE

Yanal S. Faouri, Hanin Sharif, Leena Smadi and Hani Jamleh

(Received: 15-May-2019, Revised: 23-Jun.-2019, Accepted: 9-Jul.-2019)

ABSTRACT

An electronically tunable multi-passband filter using one varactor diode is implemented based on transmission line stub method for passing several most favourable applications through multiple operating bands. In this paper, the filter is designed on Rogers RT/Duroid 5880-substrate and its input and output ports are terminated by 50 Ω *microstrip feed line. The filter passbands consist of low pass filter (LPF) with tunable cut-off frequency which can reach 0.94 GHz, then several tunable bandpass filters (BPFs) that can cover the following frequency ranges BPF1 (1.94 – 3.33 GHz), BPF2 (3.83 – 4.23 GHz), BPF3 (4.53 – 5.56 GHz) and BPF4 (6.83 – 7.48 GHz) with insertion loss (IL) of* $|S_{21}| \leq 3$ *dB. The designed filter is the binomial type with 3 elements that are implemented in three shunt stubs with the middle stub being shorted. A parametric study was conducted for the optimum location of the varactor diode and an external DC biasing circuit introduced to produce the required reverse biasing for the varactor diode and its effect was considered. The demonstrated filter is investigated using the high-frequency structure simulator (HFSS). The measured scattering parameters' S_{11} (reflection coefficient) and S_{21} (transmission coefficient) results show good agreement with the simulated values.*

KEYWORDS

Tunable filter, Reflection coefficient, Transmission coefficient, Varactor diode, Low pass filter, Bandpass filter, Bandwidth, Multiple passbands, Group delay, External quality factor, Mutual coupling.

1. INTRODUCTION

Modern microwave circuits and high-frequency applications are utilizing electronically tunable filters in order to cover more bandwidth and to be able to support multiple services. This will reduce the number of circuits used for different applications by one circuit that can support many applications and hence the complexity and system cost are reduced. In order to meet the increasing demands on rejecting out-of-band noise and jamming spectral components while simultaneously supporting multiple information channels, new developments in the design of tunable microwave filters are necessary [1]. Micro-strip filters are preferred due to their attractive features, like simplicity in manufacturing, reduction in cost, being easily integrated in circuits, high speed and high data rate capability.

Filters are tunable in many ways, including mechanical, magnetic and electronic methods. Mechanical filters are considered the best regarding power handling capability, linearity and quality factor. They have found few applications due to their huge size, low speed and large weight. Filters based on magnetic methods, like ferrimagnetic resonance, magnetostatic wave, evanescent waveguide, E-plane printed circuit and yttrium iron garnet (YIG) for providing multiple tunable bands, are preferred for higher selectivity and smaller size. On the other hand, electronic methods are done by employing semiconductors, such as PIN or varactor diodes, which can provide larger bandwidth with low IL, high selectivity, fast tuning, higher stability and lower DC biasing [2]. In contrast, micro-electromechanical systems (MEMSs) have indeed lower size, but they suffer from poor quality factor and need a large DC biasing voltage. Using MEMSs in tunable filters has been widely reported in the literature. Three-channel filter bank with two MEMS switches operates in the range 14 – 20 GHz, where each channel has a fixed three-pole end-coupled bandpass filter and the results showed an insertion loss between 1.7 and 2 dB as given in [3]. Instead of using a capacitor bank for filter tuning, it can be achieved by varying the resonator capacitive loading [4]-[5]. A single bandpass filter can also be tuned by changing the capacitive loading and hence adjusting the resonator physical size directly [6], where the filter can be tuned in the frequency range from 12 to 15 GHz with IL better than 3 dB. MEMS switches have been used as on-off elements between the resonators and the extra feed lines to form an interdigitated coplanar bandpass filter [7]; the filter can cover the range 18.5 – 21 GHz with IL less than 3.5 dB. Filters with

Y. S. Faouri*, H. Sharif, L. Smadi and H. Jamleh are with Electrical Engineering Department, Faculty of Engineering, University of Jordan, Amman, Jordan. Email: *y.faouri@ju.edu.jo

tunable characteristics employing a magnetic material such as YIG or gadolinium gallium garnet (GGG) have been utilized to design a wideband bandstop filter. Varying the magnetic field can tune the absorption occurrence and hence the center frequency rejection in the range 2.5 – 23 GHz using a microstrip line with GaAs substrate [8].

Employing varactor diodes for an electronically reconfigurable filter is another common method. A dual bandpass filter implemented using stepped impedance resonators has been reported and the center frequency tuning range for the two bands was from 0.7 – 1.2 GHz with a 3-dB fractional bandwidth (FBW) of 11.29 – 14.77 % ($\text{FBW} = 2 \times \frac{f_H - f_L}{f_h + f_L} \times 100\%$) and 1.4 – 2.15 GHz with a 3-dB FBW of 8 – 9.38 %, respectively [9]. A three-stage dual-band BPF using varactor diode and implemented using a stepped impedance method has been reported in [10] to be tuned from 1.75 – 2.66 GHz and 3.85 – 4.54 GHz with 70 MHz average bandwidth. A high-selectivity tunable dual-band bandpass filter implemented using varactor loaded resonators [11] had its first band center frequency ranging from 570 – 700 MHz with tunable 3-dB bandwidth changing from 36 – 60 MHz, while the other passband can be tuned from 1.156 – 1.336 GHz with the bandwidth varying from 67 – 85 MHz. The measured IL was from 2.3 – 2.03 dB. One tunable microstrip bandpass filter with center frequency ranging from 380 – 920 MHz and having its 3-dB bandwidth varying from 27 – 38 MHz has been reported in [12] through utilizing two varactors. Chebyshev stepped impedance filter with three shorted stubs and three varactors have been used to produce one tunable passband from 1.09 – 2.44 GHz with a reverse biased voltage changing from 0 – 30 V [13]. Combline dual bandpass filter implemented on microstrip substrate and tuned by using four varactor diodes was used to shift the center frequency from 1.85 to 1.95 GHz and from 2.1 to 2.2 GHz for the two bands, respectively [14]. The filter 3-dB bandwidth was less than 3.2 % with a tuning range of 250 MHz. Three varactors were utilized to tune the BPF lower and upper edges from 760 – 840 MHz and from 981 – 1107 MHz, respectively. The FBW was tuned from 15.5 – 36 % as reported in [15]. A BPF design using ring resonator technique with coupled feed lines was reported in [16] by using four PIN diodes as switching elements to alternate between narrowband filter and wideband filter. The 3-dB FBW could be tuned from 58.5 – 75 % at 2.4 GHz center frequency. A filter with lowpass and bandpass bands has been proposed in [17] based on three shunt stubs and loaded with a varactor diode. The LPF cut-off frequency could be tuned from 0.61 – 0.93 GHz while the bandpass was tuned from 1.85 – 3.27 GHz.

In this paper, a novel tunable planar line microwave filter design is proposed and investigated. It consists of five tunable bands; an LPF band and four BPF bands. These bands are tuned by means of varactor diode. The filter schematic and dimensions are outlined in Section 2. The proposed filter consists of three shunt stubs with varactor being connected to the middle stub for tuning the LPF cut-off frequency and the center frequency for the BPF bands. The prototype filter characteristics and the design procedure are described in Section 3. Results of simulation and discussion are presented in Section 4. The experimental verifications and a comparison with the simulated results are outlined in Section 5. Finally, the conclusion is given in Section 6.

2. FILTER STRUCTURE

The proposed filter consists of three shunt stubs with 50 Ω input and output feed lines; the first and third stubs are open-circuited, while the second stub is short-circuited. The low passband and quad bandpass regions are created with acceptable impedance bandwidth and IL at the passband and good S_{11} values at the pass frequencies by adjusting the length and width of the three stubs, the location of the varactor and the DC biasing circuit element value. The geometrical parameters for the proposed filter are shown in Figure 1, where all dimensions are carefully obtained by parametric analysis in order to achieve the desired response over the needed frequency range. The overall filter dimensions are $5.1 \times 10.8\ \text{cm}^2$. It is fabricated on a double-side Rogers RT/Duroid 5880 substrate with tan δ = 0.0009 and ε_r = 2.2 with 0.8 mm thickness. The supply positive and negative terminals are connected to the varactor cathode and anode, respectively. The footprint for the inductor and resistor has been taken as $1.2 \times 0.6\ \text{mm}^2$, while for the varactor, it is $1 \times 0.8\ \text{mm}^2$ and the other filter parameters are listed in Table 1.

Table 1. Dimensions for the proposed filter geometry in mm.

W1 = 23	W2 = 62	W3 = 1.2	W4 = 12	Substrate width = 51
L1 = 2.5	L2 = 1.2	L3 = 44.125	L4 = 22	Substrate length = 108

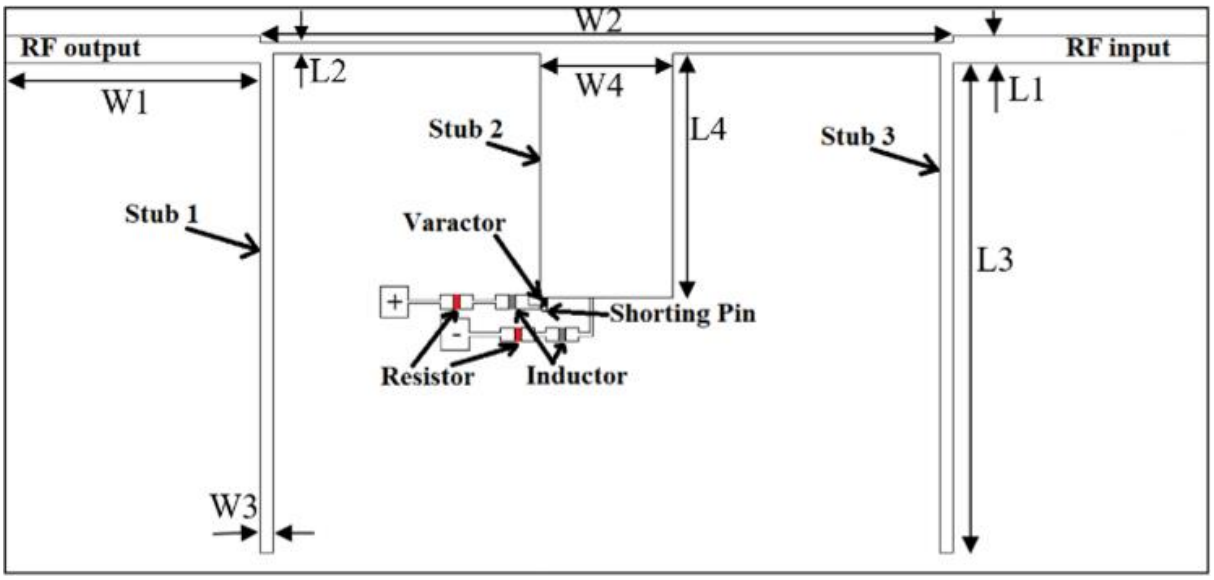

Figure 1. The proposed filter geometry with two open-circuited stubs and one short-circited stub.

3. DESIGN PROCEDURE

The design starts with a maximally flat LPF prototype consisting of three elements based on the IL method. The lumped circuit elements of the low-pass prototype filter are found to be $g_o = 1, g_1 = 1, g_2 = 2, g_3 = 1, g_4 = 1$. The prototype filter is modified to act as a bandpass filter by transforming every element of the LPF to a combination of an inductor and capacitor [18].

The bandpass filter with lumped elements is implemented using a microstrip transmission line model, which is done using the Kuroda Identities (first and second kinds) and Richards' transformations (to convert the lumped elements into transmission lines). The resulting stub dimensions have been calculated based on the chosen substrate and considering the open or short termination of the transmission line stubs that act as resonators.

The varactor type SMV1232, which is a hyper-abrupt junction, tunes the varactor from Skyworks [19] that works under a reverse biasing voltage varying between 0 – 15 V and can provide an appropriate quality factor 'Q' in wireless systems for frequencies over 10 GHz. It is being inserted to change the filter overall capacitance and hence the resonant frequency of the band will change accordingly.

4. RESULTS AND ANALYSIS

The proposed filter was simulated using HFSS and several parametric studies have been conducted to achieve a filter with multi-pass bands which cover many highly demanded services. The filter first band covers low frequencies and its cut-off frequency can be tuned from 710 to 940 MHz. It can be used to pass LTE 700, GSM 3G 800, GSM 3G 900, industrial, scientific and medical (ISM) applications. At 200 MHz and beyond from the cut-off frequency, the attenuation can reach 50 dB.

The second passing filter is a bandpass filter BPF1 which is tuned from 1.94 – 3.33 GHz with FBW ranging from 2.74 – 8.4 % as the biasing voltage decreases and it has an average BW of 155 MHz while being tuned. This band can be utilized to pass many services, such as; wireless fidelity (Wi-Fi), Bluetooth, GSM 2100 and GSM 2300. This band has low IL varying from 0.38 – 0.98 dB. The third passband BPF2 covers frequencies from 3.83 – 4.23 GHz with FBW 1.55 – 9.93 % for a reverse biasing voltage form 3 – 15 V with an IL $\leq$ 3 dB, whereas below 3 V, the filter has a relatively higher loss that can reach 7 dB. The tuning BW for this passband ranged from 60 to 400 MHz with an average of 263 MHz. This band can be used for worldwide interoperability for microwave access (Wi-MAX) applications. The fourth band BPF3 ranges from 4.62 – 5.56 GHz with an average BW of 397 MHZ and it is suitable for C-band uplink and downlink and Wi-Fi applications and its FBW can be tuned from 5.54 – 15.38 %. The last passing band BPF4 has an average BW of 366 MHz and can cover frequencies from 6.85 – 7.43 GHz, which makes it suitable for satellite communications with FBW tuned from 6.64 – 8.12 %. The cut-off frequency for the LPF and the upper 'f_H' and lower 'f_L' frequencies for the four

passbands are listed in Table 2. Some cases for which the IL ≥ 3 dB in the BPF2 band are identified in Table 2.

Table 2. Proposed filter passing frequencies for all varactor capacitance values.

Varactor	LPF	BPF 1		BPF 2		BPF 3		BPF 4	
C (pF)	f_C (GHz)	f_L (GHz)	f_H (GHz)	f_L (GHz)	f_H (GHz)	f_L (GHz)	f_H (GHz)	f_L (GHz)	f_H (GHz)
4.15	0.71	1.94	2.11	IL is higher than 3dB		4.62	5.39	6.85	7.43
3.22	0.80	2.07	2.28			4.53	5.18	6.97	7.28
2.67	0.84	2.18	2.43			4.47	4.97	6.91	7.34
2.28	0.87	2.29	2.54			4.71	5.38	6.74	7.40
1.97	0.89	2.41	2.66			4.74	5.37	6.88	7.48
1.72	0.89	2.54	2.78			4.41	4.90	6.92	7.36
1.51	0.91	2.65	2.87	3.83	3.89	4.79	5.38	6.83	7.40
1.35	0.91	2.76	2.96	3.83	3.92	4.80	5.35	6.96	7.24
1.22	0.92	2.86	3.03	3.83	3.95	4.85	5.36	6.91	7.22
1.13	0.92	2.93	3.09	3.83	3.99	4.93	5.43	6.83	7.27
1.05	0.93	2.99	3.14	3.83	4.02	4.96	5.42	6.92	7.27
0.99	0.93	3.04	3.18	3.83	4.05	5.05	5.48	6.91	7.29
0.94	0.93	3.08	3.21	3.82	4.06	5.07	5.48	6.94	7.27
0.90	0.93	3.10	3.23	3.83	4.09	5.02	5.38	6.93	7.29
0.86	0.93	3.14	3.25	3.83	4.11	5.06	5.43	6.99	7.20
0.84	0.93	3.16	3.27	3.83	4.12	5.11	5.48	6.91	7.27
0.81	0.93	3.17	3.28	3.83	4.15	5.09	5.42	6.93	7.21
0.78	0.94	3.21	3.31	3.83	4.18	5.20	5.54	7.01	7.31
0.76	0.94	3.22	3.32	3.83	4.19	5.23	5.54	6.93	7.34
0.75	0.94	3.22	3.32	3.83	4.21	5.22	5.54	6.84	7.33
0.74	0.94	3.23	3.32	3.83	4.21	5.26	5.55	6.96	7.34
0.73	0.94	3.24	3.33	3.83	4.21	5.22	5.53	6.99	7.30
0.72	0.94	3.24	3.33	3.83	4.23	5.26	5.56	6.84	7.31

The required coupling parameters are the external quality factor (Q_e) and the mutual coupling and they are displayed in Figure 2 for BPF1 and BPF3. It can be shown that the proposed filter has high Q_e and lower mutual coupling. External quality factor describes the amplitude at resonance and is calculated using Equation 1, while mutual coupling determines the spacing required between adjacent elements and is calculated using Equation 2.

$$Q_{ei}^{(n)} = \frac{g_i g_{i+1}}{(FBW)_n} \tag{1}$$

$$M_{i,i+1}^{(n)} = \frac{(FBW)_n}{\sqrt{g_i g_{i+1}}} \tag{2}$$

where FBW is defined earlier in Section 1, ‘n’ is the number of the pass band (n = 1, 2, 3, 4) and ‘i’ is

an index for the LPF prototype element (i = 0, 1, 2, 3, 4) given in Section 3. From the equations above, $Q_{e1}^{(n)} = Q_{e4}^{(n)}$, $Q_{e2}^{(n)} = Q_{e3}^{(n)}$ and $M_{12}^{(n)} = M_{23}^{(n)}$.

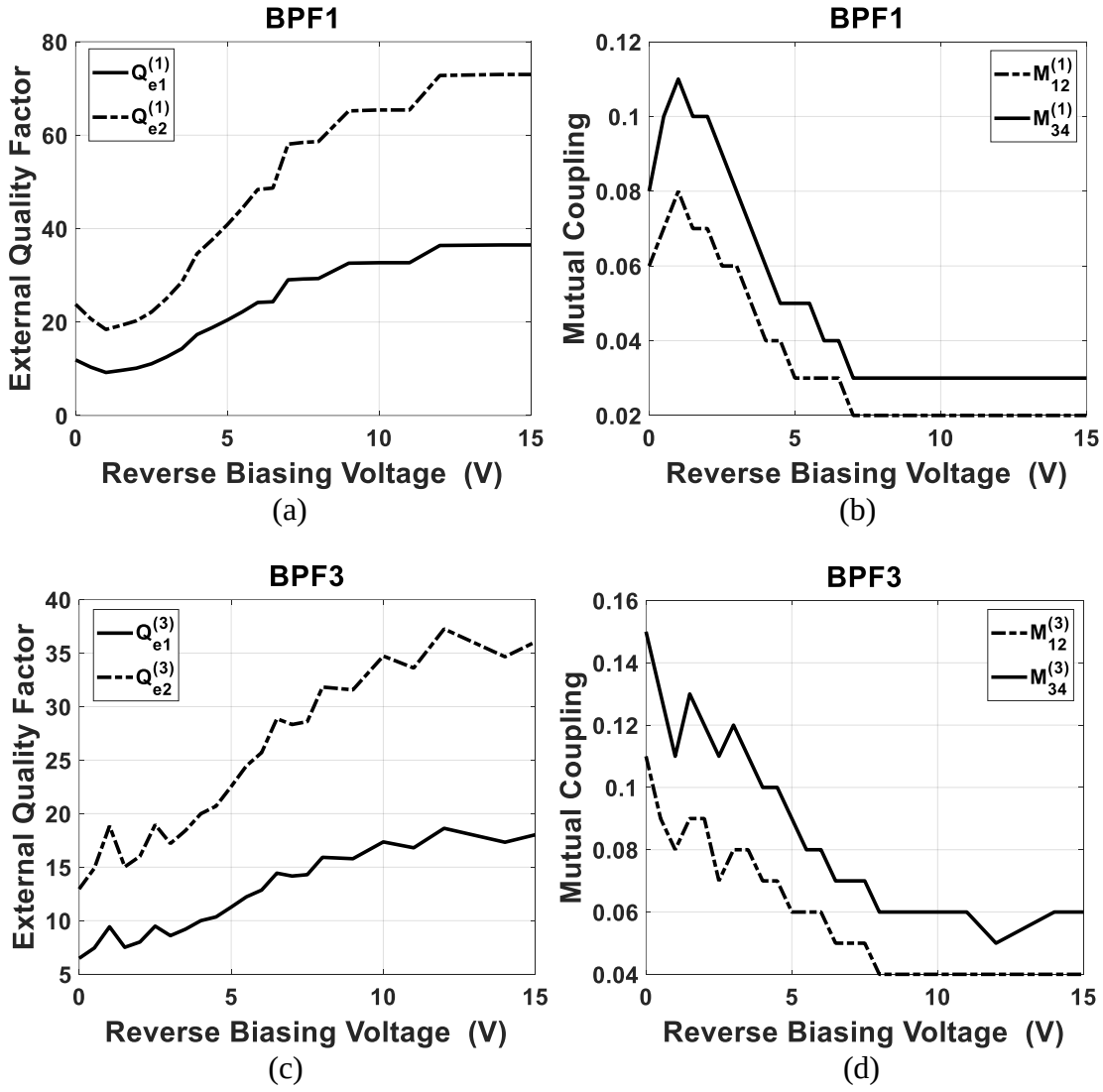

Figure 2. Filter parameters (a) external quality factor for BPF1 (b) Mutual coupling for BPF1, (c) external quality factor for BPF3 and (d) Mutual coupling for BPF3.

Scattering parameters S_{21} and S_{11} are the most important filter characteristics which display the utilized or rejected frequencies. The previously explained bands can be noticed from S_{21} and S_{11} curves shown in Figure 3 and Figure 4, respectively for selected varactor capacitances. The return loss (RL) within the passband is greater than 15 dB for all tuning states.

It can be noticed from Figure 3 that the filter has two fixed transmission zeros between BPF1 and BPF2 bands and between BPF3 and BPF4 bands, while the filter has two tunable transmission zeros (TZs) located between the LPF and BPF1 bands and between the BPF2 and BPF3 bands.

The current distribution shown in Figure 5 demonstrates the part of the filter which is active at the selected frequency through monitoring the filter element that has the highest surface current which is 50 A/m. At a frequency of 10 MHz, which is in the LPF band, the input and the output and the transmission line connecting the stubs are responsible for this mode of operation as shown in Figure 5(a). For a frequency of 1.23 GHz, which belongs to the rejected band, it can be noticed that most of the filter has no current passing through, since the signal was inserted from the right port to the left port and was reflected and dissipated through the first stub as can be noticed from Figure 5(b). At 2.14 GHz, which is the center frequency for the bandpass filter mainly, the first stub is responsible for this band named BPF1 as shown in Figure 5(c). For the second passband named BPF2, the current distribution is shown in Figure 5(d), where the middle and third stubs are active at 4 GHz. At a frequency of 4.49 GHz, which

belongs to the BPF3, the filter middle stub is responsible as shown in Figure 5(e) and for the BPF4 at 7.15 GHz, the whole filter except the shorted stub has higher maximum surface current with higher order modes being transmitted in the transmission lines as shown in Figure 5(f).

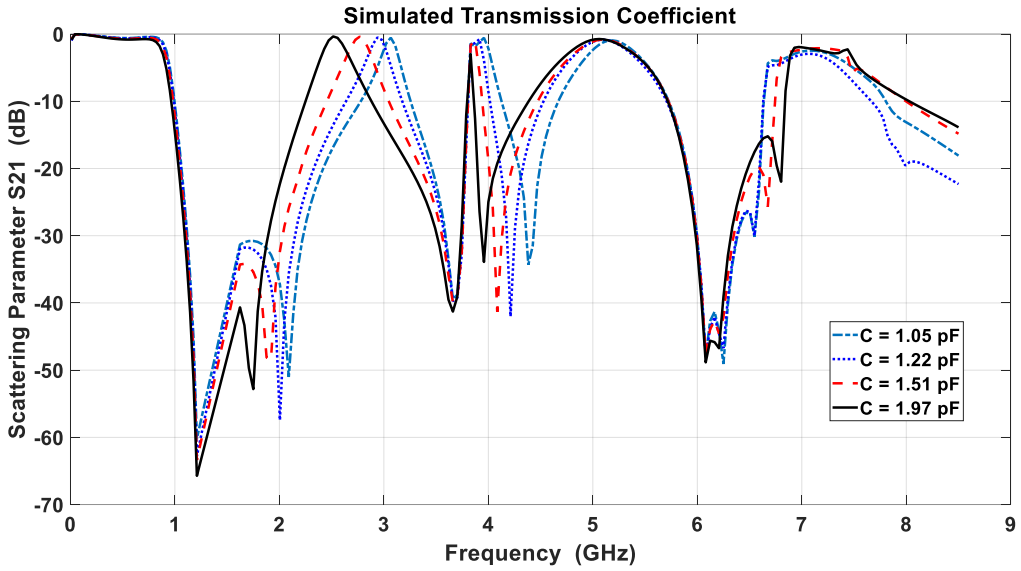

Figure 3. Simulated transmission coefficients for various varactor capacitances.

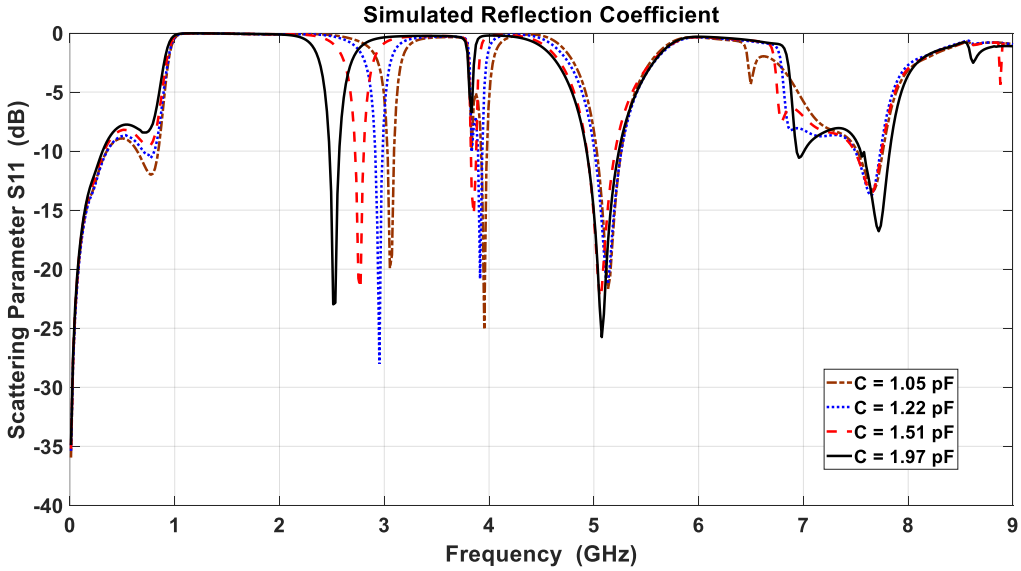

Figure 4. Simulated reflection coefficients for various varactor capacitances.

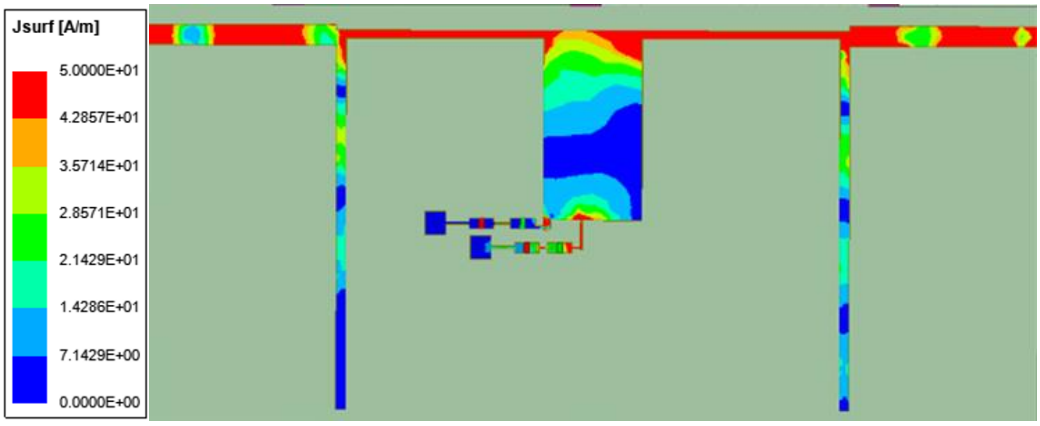

(a)

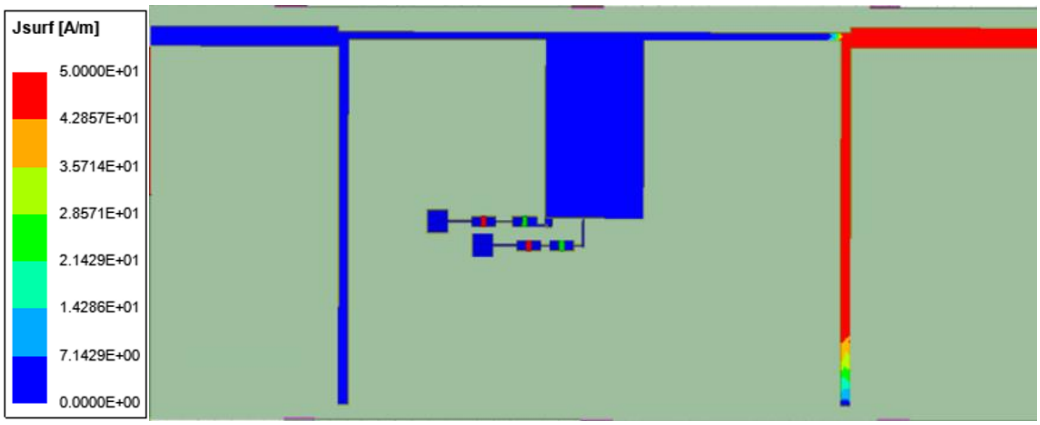
Jsurf [A/m]
5.0000E+01
4.2857E+01
3.5714E+01
2.8571E+01
2.1429E+01
1.4286E+01
7.1429E+00
0.0000E+00

(b)

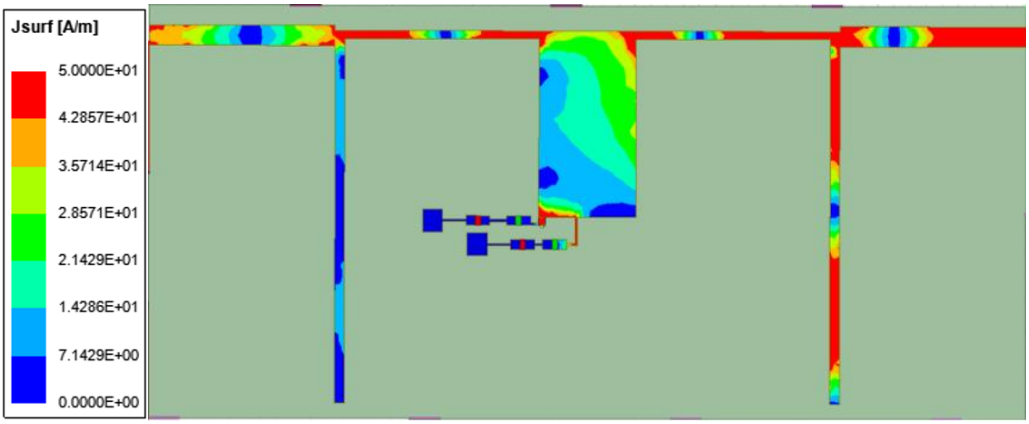
Jsurf [A/m]
5.0000E+01
4.2857E+01
3.5714E+01
2.8571E+01
2.1429E+01
1.4286E+01
7.1429E+00
0.0000E+00

(c)

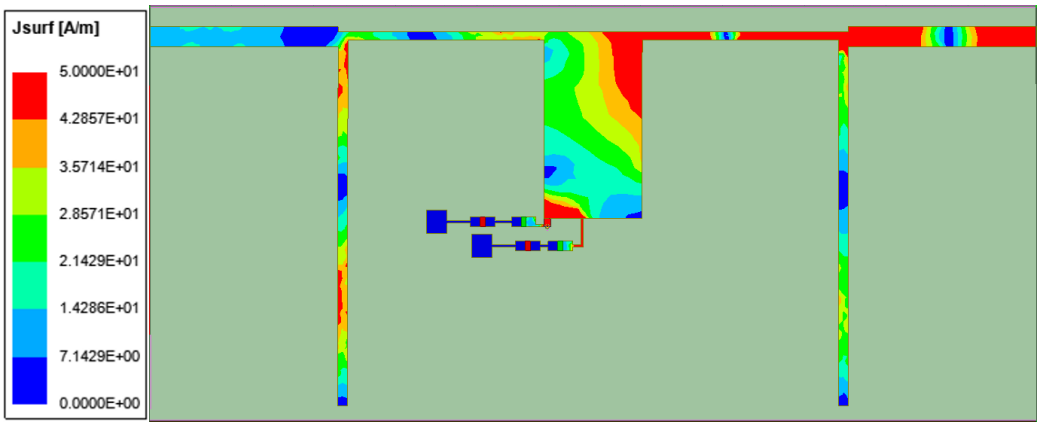
Jsurf [A/m]
5.0000E+01
4.2857E+01
3.5714E+01
2.8571E+01
2.1429E+01
1.4286E+01
7.1429E+00
0.0000E+00

(d)

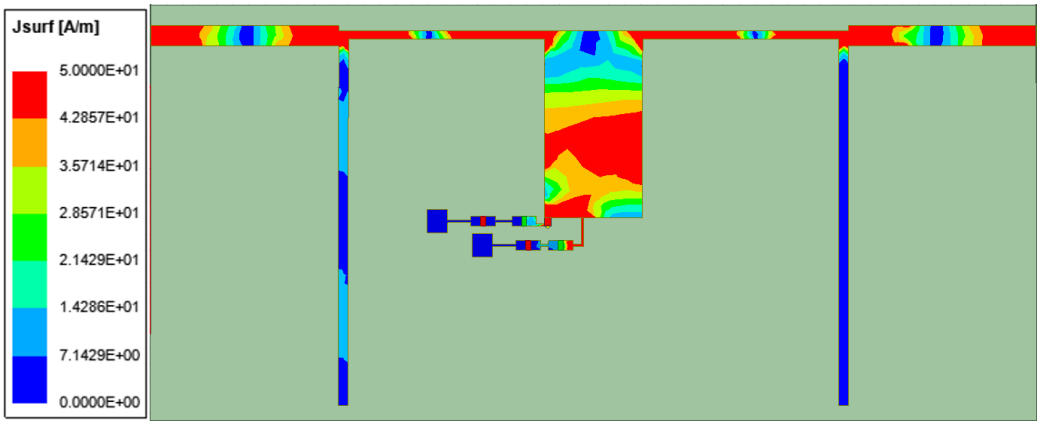
Jsurf [A/m]
5.0000E+01
4.2857E+01
3.5714E+01
2.8571E+01
2.1429E+01
1.4286E+01
7.1429E+00
0.0000E+00

(e)

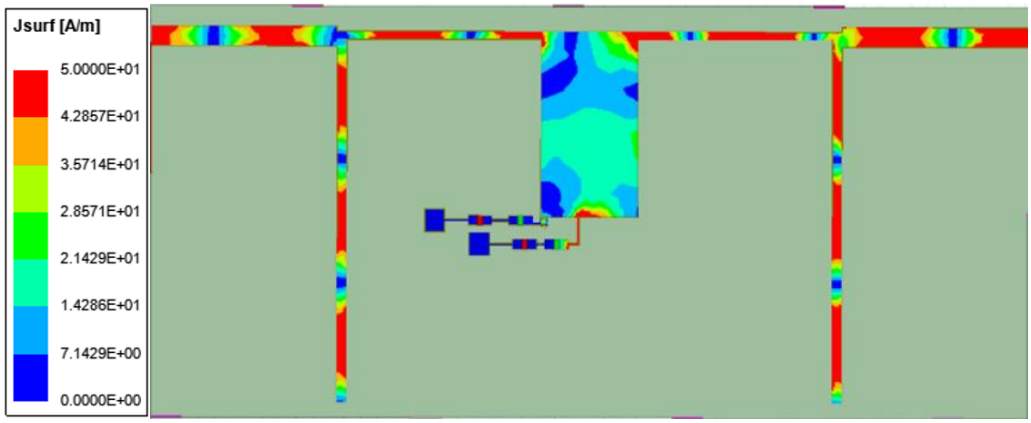

(f)

Figure 5. The simulated surface current distribution at frequencies (in GHz): (a) 0.01, (b) 1.23, (c) 2.14, (d) 4, (e) 5 and (f) 7.15.

Group delay is one of the filter's important characteristics. The simulated results for the first bandpass band are shown in Figure 6. The group delay changes tend to decrease by reducing the capacitance and its maximum value is 2.5 ns at 0 V, where the diode has the largest capacitance value of 4.15 pF.

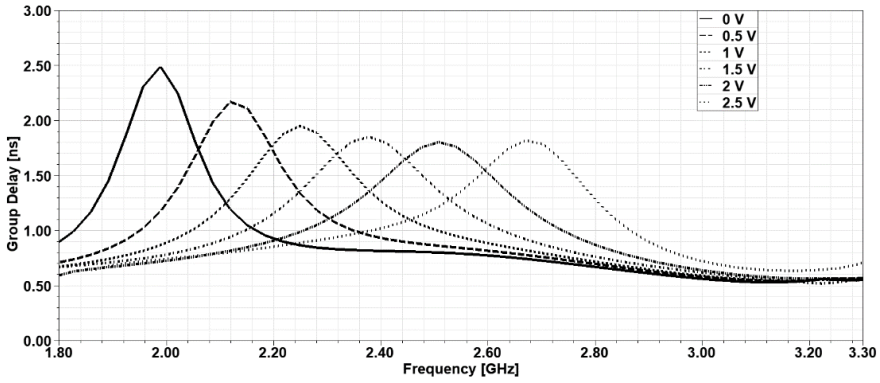

Figure 6. Group delay for the BPF 1st band.

Comparison between the proposed filter and different filters reported in published research that have been tuned using varactors regardless of the filter shape or the used elements to create the passing bands, is given in Table 3. The proposed filter has the largest number of passing bands compared to all other reported filters.

Table 3. Comparison between the proposed filter and filters presented in other published works.

Parameter / Reference	Filter bands	No. of zeros	Tuning bands	FBW (%)	Side rejection (dB)	No. of varactors	Min. IL (dB)	Size (mm^3) (in λ^2)
[9]	BPF	3	2	11.29 – 14.77 8 – 9.38	> 40	6	3.86	$19 \times 33.35 \times 0.79$ $(0.07\lambda \times 0.16\lambda)$
[11]	BPF	4	2	6.5 – 8.5 5.8 – 6.4	> 30	4	2.32	$11.5 \times 19 \times 0.81$ $(0.04\lambda \times 0.07\lambda)$
[12]	BPF	2	1	4.1 – 7.1	> 50	2	5.0	$25 \times 35 \times 1.524$ $(0.06\lambda \times 0.08\lambda)$
[13]	BPF	2	1	16.5 – 37.7	> 50	3	~ 4.5	$30 \times 54 \times 0.508$ $(0.19\lambda \times 0.34\lambda)$
[14]	BPF	2	1	13.1 – 16.3	> 40	4	~ 4.0	$40 \times 40 \times 0.8$ $(0.44\lambda \times 0.44\lambda)$
Proposed	**LPF & BPF**	6	**5**	2.74 – 8.4 1.55 – 9.93 5.54 – 15.38 6.64 – 8.12	> 30	**1**	**0.38**	$52 \times 108 \times 0.8$ $(0.17\lambda \times 0.35\lambda)$

The number of zeros is introduced to show that these passbands are not harmonics of the first passband by noticing that all our passbands have an insertion loss lower than 3 dB with a lower sideband rejection greater than 30 dB over the entire considered frequency range. The proposed filter has a large substrate size compared to [9]-[11], because it is passing lower frequencies but is still small if measured in terms of the guided wavelength. The guided wavelength is calculated based on the lowest -3 dB intersection. It has the best IL values at the band center frequency compared to all the reported filters. Furthermore, the proposed filter has utilized only one varactor diode.

5. EXPERIMENTAL VERIFICATION

The designed filter is fabricated on an RT/Duroid 5880 substrate with a dielectric constant $\varepsilon_r = 2.2$ and height $h = 0.8$ mm as shown in Figure 7. The filter reflection and transmission coefficients have been measured by means of the vector network analyzer (Rohde & Schwartz ZNB8) [20] and are displayed in Figure 8 and Figure 9, respectively. The measured IL for BPF1 is from 0.76 – 2.44 dB and for BPF2 is from 0.78 – 2.94 dB. The parasitic resistor of the varactor accounts for this IL. The measured S_{21} and S_{11} compare favourably with the simulated results.

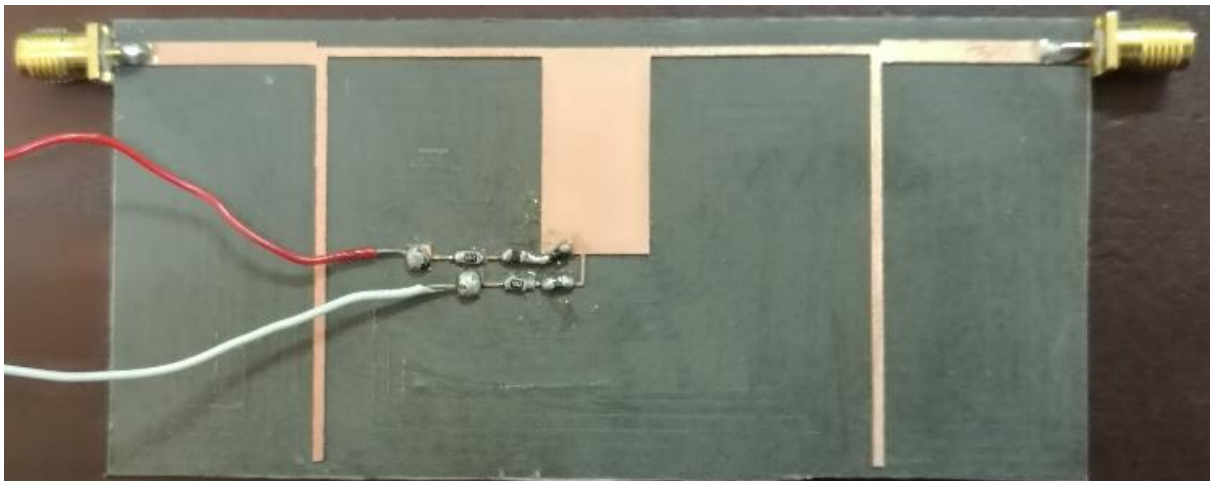

Figure 7. The fabricated filter with the DC biasing circuit.

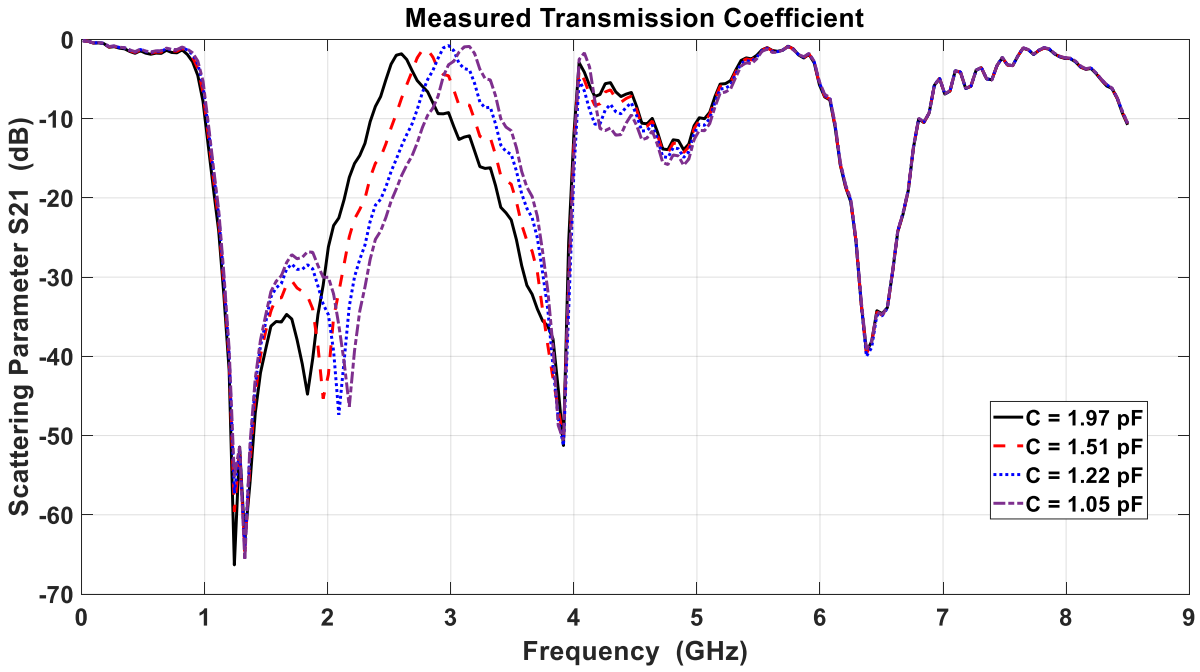

Figure 8. Measured transmission coefficients for various varactor capacitances.

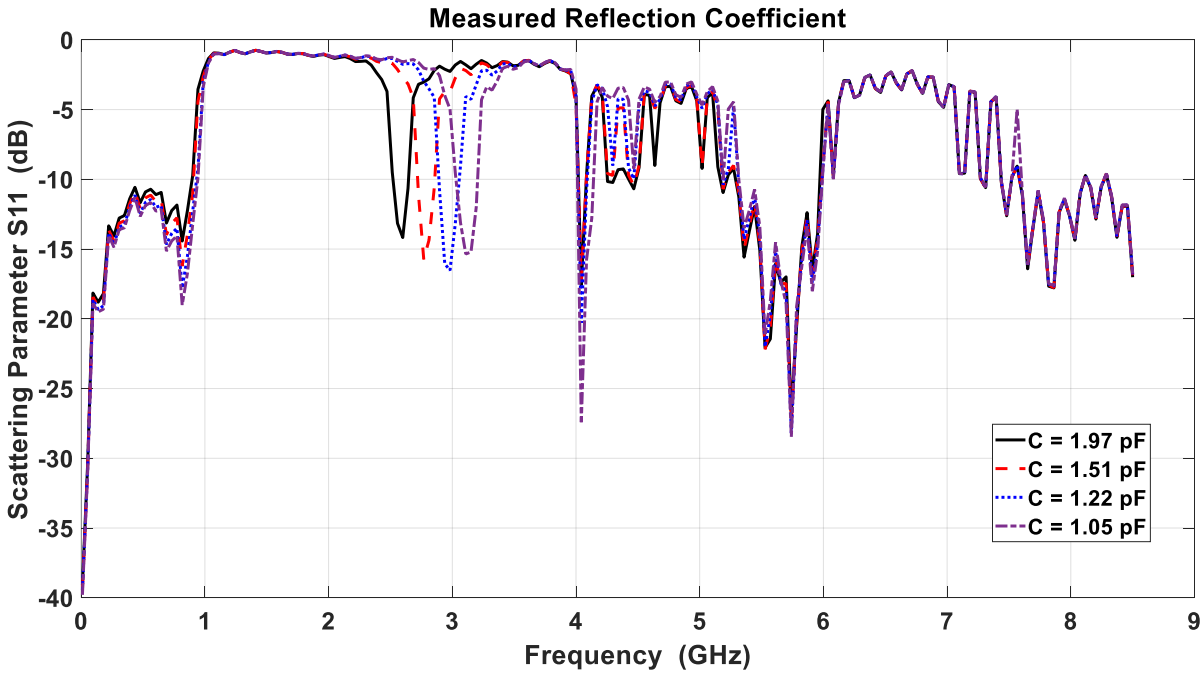

Figure 9. Measured reflection coefficients for various varactor capacitances.

The simulated and measured reflection coefficient results for the proposed filter under 2 V biasing voltage are shown in Figure 10 and they compare favourably. A comparison between the simulated and measured results is shown in Table 4. The differences between measured and simulated results are due to different factors which are not considered through the simulation process, such as the accuracy and precision of fabrication techniques used, the SMA connector welding, the non-homogeneous behaviour of the RT/Duroid substrate with frequency variations as well as the varactor behaviour with frequency. Varying the reverse biasing voltage will cause varactor capacitance to change and hence the center frequency and the bandwidth chane as well. The simulated and measured variation of the center frequency for the BPF1 with the reverse biasing is shown in Figure 11 (a).

The resonant frequency increases with increased reverse voltage. The bandwidth behaviour for the simulated and measured results with the varactor capacitance is shown in Figure 11 (b).

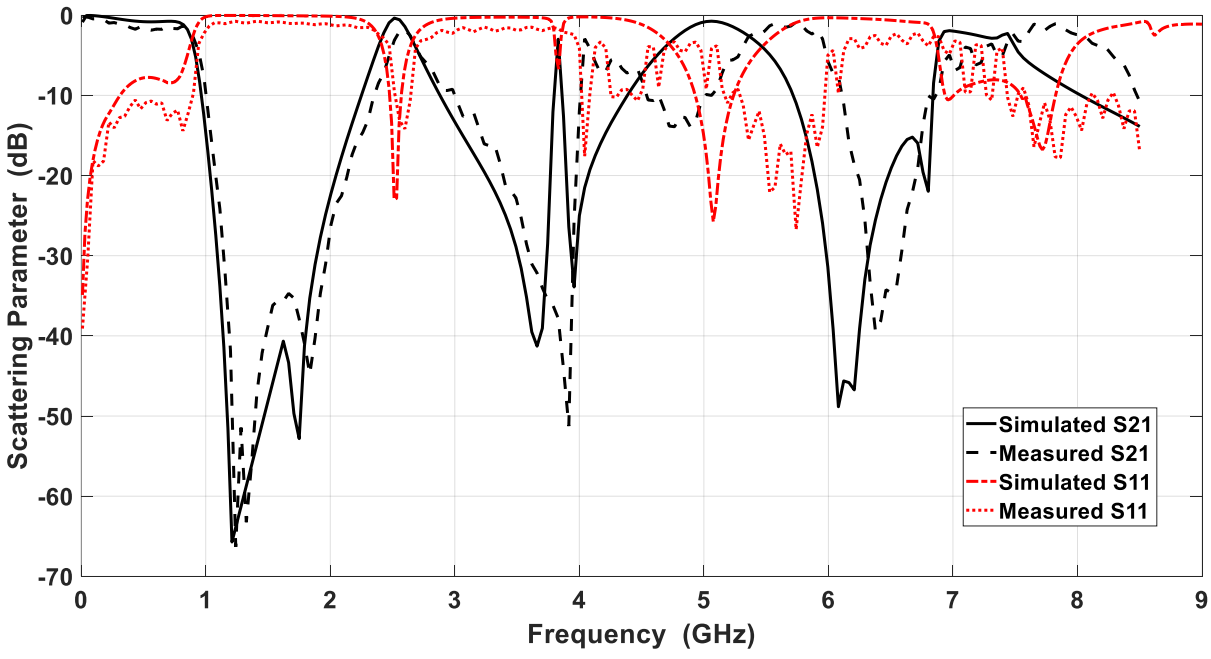

Figure 10. Simulated and measured S_{11} and S_{21} for C = 1.97 pF (V_R = 2 V).

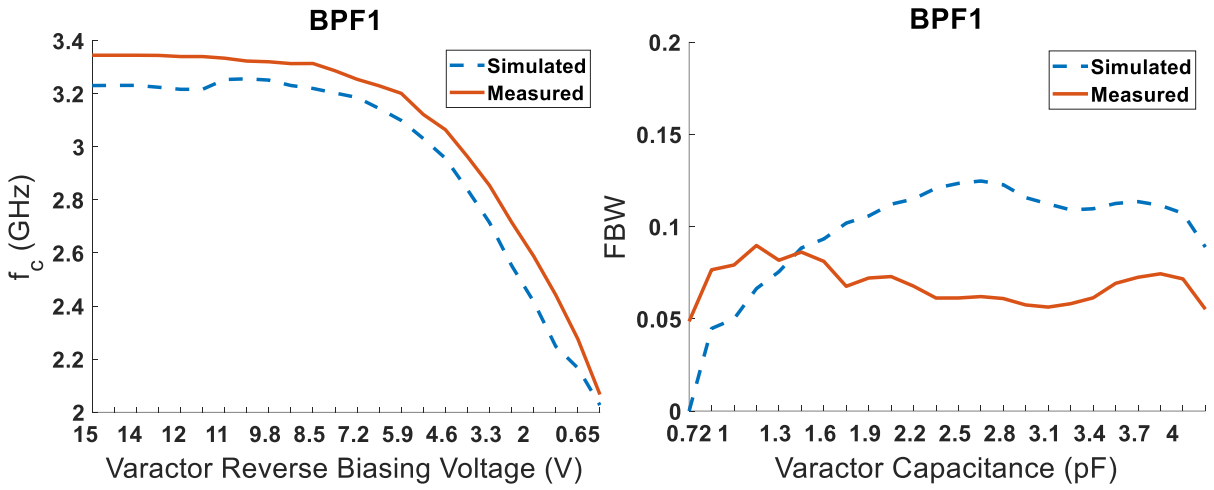

(a) (b)

Figure 11. Simulated and measured results; (a) filter BPF1 center frequency *vs.* biasing voltage, (b) BPF1 fractional bandwidth *vs.* varactor capacitance.

Table 4. Comparison between simulated and measured results.

	Simulation			Measurement		
	Max IL dB	**Tuning Range GHz**	**Zero level after the band**	**Max IL dB**	**Tuning Range GHz**	**Zero level after the band**
LPF	---	0.71 – 0.94	-60	---	0.61 – 0.74	-53
BPF1	0.94	1.94 – 3.33	-39	2.44	2 – 3.4	-33
BPF2	1.24	3.83 – 4.23	-33	1.7	4 – 4.35	-22
BPF3	1.33	4.53 – 5.56	-36	1.83	5.35 – 5.95	-39
BPF4	1.8	6.83 – 7.48	---	2.3	7.4 – 8.15	---

6. CONCLUSION

A new planar enhanced tunable filter is designed for multi-band applications. The proposed filter consists of three stubs with two being open-circuited and a short-circuited stub in the middle that is connected to the ground through a shorting pin. A DC circuitry has been considered and implemented for the design of proper biasing of the varactor diodes. The design is investigated using HFSS. The simulation results show good impedance matching over the passing frequencies for RL $\geq$ 15 dB and lower insertion losses IL $\leq$ 3 dB. Results of measurements and simulation for the transmission and reflection coefficients compare favourably. Current distribution at different selected frequencies has been viewed to clarify the filter behaviour. The filter group delay is lower than 3 ns. This kind of filters could be useful in future reconfigurable RF front-end systems for radars and wireless communication systems.

ACKNOWLEDGEMENTS

The authors acknowledge the valuable support of the technical staff of the Tech Works (super Fab lab) located in the King Hussein Business Park (KHBP) through the performed fabrication of the proposed filter.

REFERENCES

[1] P. W. Wong and I. Hunter, "Electronically Tunable Filters," IEEE Microwave Magazine, vol. 10, no. 6, pp. 46–54, 2009.

[2] J. Uher and W. J. R. Hoefer, "Tunable Microwave and Millimeter-wave Band-pass Filters," IEEE Transactions on Microwave Theory and Techniques, vol. 39, no. 4, pp. 643–653, 1991.

[3] I. C. Reines et al., "A Low Loss RF MEMS Ku-band Integrated Switched Filter Bank," IEEE Microw.

Wirel. Components Lett., vol. 15, no. 2, pp. 74–76, 2005.

[4] C. A. Hall, R. C. Luetzelschwab, R. D. Streeter and J. H. Vanpatten, "A 25 Watt RF MEM-tuned VHF Bandpass Filter," Proc. of IEEE MTT-S International Microwave Symposium Digest, pp. 503–506, 2003.

[5] J. H. Park, H. T. Kim, Y. Kwon and Y. K. Kim, "Tunable Millimeter-wave Filters Using a Coplanar Waveguide and Micromachined Variable Capacitors," Journal of Micromechanics and Microengineering, vol. 11, no. 6, pp. 706–712, 2001.

[6] A. Pothier et al., "Low-loss 2-Bit Tunable Bandpass Filters," IEEE Transactions on Microwave Theory and Techniques, vol. 53, no. 1, pp. 354–360, 2005.

[7] E. Fourn et al., "MEMS Switchable Interdigital Coplanar Filter," IEEE Transactions on Microwave Theory and Techniques, vol. 51, no. 1, pp. 320–324, 2003.

[8] C. S. Tsai, "Wideband Tunable Microwave Devices Using Ferromagnetic Film-gallium Arsenide Material Structures," Jou. Magn. Magn. Mater., vol. 209, no. 1–3, pp. 10–14, 2000.

[9] X. Zhang, C. Chen, M. Li, L. Zhou and B. Liu, "A Compact Tunable Dual-band Bandpass Filter Using Varactor-loaded Step-impedance Resonators," PIERS Proceedings, vol. 1, pp. 2642–2645, Prague, Czech Republic, 2015.

[10] L. Smadi, H. Sharif and Y. S. Faouri, "Dual-Band Tunable Microwave Bandpass Filter Using Stepped Impedance Technique," Proc. of IEEE Jordan Int. Jt. Conf. Electr. Eng. Inf. Technol., pp. 827–830, Apr. 2019.

[11] X. Y. Zhang, L. Gao, Y. Cao, X.-L. Zhao and Y. Ding, "Independently-tuned Dual-band Filter Using Varactor-loaded Resonators," Prog. Electromagn. Res. C, vol. 42, no. May, pp. 55–66, 2013.

[12] A. Golaszewski, M. Zukocinski and A. Abramowicz, "Design of Varactor Tuned Bandpass Filter," Proc. of the 14th Conf. Microw. Tech. Com., pp. 86–89, 2015.

[13] Y. Guan and Q. Guo, "A Varactor-tuned Bandpass Filter Based on Lowpass Filter and Shorted Stubs," Microw. Opt. Technol. Lett., vol. 56, no. 4, pp. 879–883, 2014.

[14] B. Kim and S. Yun, "Varactor-Tuned Combline Bandpass Filter," IEEE Trans. Microw. Theory Tech., vol. 52, no. 4, pp. 1279–1283, 2004.

[15] Y. Shang, W. Feng and W. Che, "Wideband Reconfigurable Bandpass Filter Using Coupled Lines Loaded with Varactor Loaded Stubs," Int. J. RF Microw. Comput. Eng., vol. 28, no. 2, 2018.

[16] S. Arain, P. Vryonides, M. A. B. Abbasi, A. Quddious, M. A. Antoniades and S. Nikolaou, "Reconfigurable Bandwidth Bandpass Filter with Enhanced Out-of-Band Rejection Using π-Section-loaded Ring Resonator," IEEE Microw. Wirel. Components Lett., vol. 28, no. 1, pp. 28–30, 2018.

[17] H. Sharif, L. Smadi and Y. S. Faouri, "Stub Resonator Tunable Bandpass and Lowpass Filters Using Shunt Stub Resonators," Proc. of IEEE Jordan Int. Jt. Conf. Electr. Eng. Inf. Technol., pp. 442–445, Apr. 2019.

[18] D. M. Pozar, Microwave Engineering, 4th Edition, New York: Wiley, 2012.

[19] Skyworks Solutions, "SMV123x Series : Hyperabrupt Junction Tuning Varactors," [Online], Available at: http://www.skyworksinc.com/uploads/documents/200058Q.pdf, 2012.

[20] W. D. Reeve, "Filter Measurements with a Vector Network Analyzer," pp. 1–16, [Online], Available at: http://www.reeve.com/Documents/Articles%20Papers/Reeve_FilterMeasVNA.pdf, 2016.

Jordanian Journal of Computers and Information Technology (JJCIT), Vol. 05, No. 02, August 2019.

ملخص البحث:

تم تصميم مرشِّح قابل للضبط الكترونياً لتمرير عددٍ من النطاقات الترددية والذي يستخدم ثنائياً متغير المواسعة وتنفيذه بناءً على تقنية رنين الصَّدم، وذلك من أجل تمرير عدة تطبيقاتٍ مفضّلة عبر نطاقات تشغيل ترددية متعددة.

في هذه الورقة، تم تصميم المرشِّح بحيث كان طرفا مدخله ومخرجه مزوَّدين بخط تغذية شريطي صغير مقاومته (50) أوم. أما النطاقات الترددية التي صُمّم المرشِّح لتمريرها فهي: نطاق للترددات المنخفضة بتردد قطع قابل للضبط بحيث يصل الى (0.94) جيجاهيرتز، بالإضافة الى عدد من النطاقات الترددية الأخرى التي تتراوح تردداتها بين 1.94-3.3 جيجاهيرتز للنطاق الأول، وبين 3.83-4.23 جيجاهيرتز للنطاق الثاني، وبين 4.53- 5.56 جيجاهيرتز للنطاق الثالث، وبين 6.83-7.48 جيجاهيرتز للنطاق الرابع. أما فقد الإدخال للمرشِّح عند تلك الترددات، فهو يقلّ عن (3) ديسيبل. والجدير بالذكر أن المرشِّح المصمم في هذه الدراسة هو من النوع ذي الحدَّين، ويتضمن (3) عناصر منفّذة في شكل صَدّامات توازٍ بحيث تكون الصدّامة الوسطى في حالة قِصَر.

وقد أجريت دراسة لتحديد الموضع المثالي للثنائي متغير السعة، واستخدم مصدر خارجي لتوفير الانحياز العكسي المطلوب للثنائي متغير السعة وأخذ تأثيره بعين الاعتبار. وتم استخدام محاكي بِنية التررددات العالية (HFSS) لدراسة المرشِّح المصمم في هذه الدراسة. وكانت النتائج المقاسة المتعلقة بمعاملات التشتت (معامل الانعكاس ومعامل الارسال) متفقة بصورة جيدة مع القيم التي تم الحصول عليها عن طريق المحاكاة.